FreeHydroCells

D1.1

Report findings on the growth and structural, chemical, and physical characterization of TCO, TMD materials, and substrates, version 1

WP 1. TMD/TCO Materials: Materials and Processing Development and Characterisation

Status: Final

31 October 2024

Grant Agreement No 101084261

Funded by the European Union

Document Information

Title	Report findings on the growth and structural, chemical and physical characterization of TCO, TMD materials, and substrates, version 1
Dissemination Level	Public
Deliverable Leader	CNR
Type	R - Document, report
Contributing Authors (Name, Organisation)	Salvatore Antonino Lombardo (CNR), Ulrich Plachetka (AMO), Desislava Daskalova AMO), Ian Povey (UCC), Jun Lin (UCC), Ailbe Ó Manacháin (UCC), Vikas Jangra (RWTH)

Funding

This project has received funding from the European Union under grant agreement No 101084261.

Disclaimer

Contents

Executive Summary

The effect of climate change on the Earth has become critical. We must find a way to reduce and ultimately replace the necessity for burning fossil fuels to extract our energy needs in order to reduce the level of pollutants from such processes entering the atmosphere and driving global warming with the related negative consequences for the environment and humanity globally. Many “green” energy conversion solutions (with no pollutant byproducts) have been investigated to date, including wind, wave and solar. Significant bottlenecks in achieving high conversion efficiency, low-cost production and operation, low maintenance cost, long and stable product life, energy storage and material sustainability have significantly reduced the ability of these potentially green solutions to challenge – both practically and financially – the dominant and pollutant-rich fossil fuel energy extraction methods.

The FreeHydroCells project is designated by the European Commission as a high-risk / high-reward (if fully successful) project that has very specific objectives aimed at addressing these top level bottlenecks by adopting a radical and novel approach of employing environmentally-benign sustainable materials to form a stable, high-efficiency/low-cost, water splitting system driven by sunlight absorption in a buried multijunction cell-based system. The following phrase sums up our consortium’s approach to achieving a novel energy solution, “*It must be entirely green (pollutant-free), very lean (highly efficient in energy conversion) and broadly mean (low-cost, sustainable, stable, storable) to enable a novel energy dream (of having the potential to challenge the dominance of pollutant-rich energy conversion processes)*”.

The FreeHydroCells project is presently approaching the end of Month 24 of 40 in the project timeline. The present D1.1 deliverable report is focused on providing a public dissemination level summary of the work to date on the potential building block TCO and TMD materials realized and structurally investigated by the consortium in Work Package 1 of the project (TMD/TCO Materials: Materials and Processing Development and Characterisation) to meet Milestone 2.

This material building block assessment in Work Package 1 plays an important part in developing the sources for the material integration of forming multijunction material systems in Work Package 2 (TMD/TCO BMJ PEC cells: Application of Materials and Processing Developments for Realising BMJ PEC Cells, Optimisation and Characterisation) in order to form buried multijunction photoelectrochemical cells to split water and make green molecular (diatomic) hydrogen fuel. The FreeHydroCells project adopts an iterative (symbiotic-like) process interrelationship between the four technical Work Packages, including between WP 1 and WP 2. Therefore, the material building block assessment not only guides the direction of activities in WP 2, it also is influenced by the feedback findings from WP 2.

The report is divided in three parts:

(1) Task 1.1 (TCO layer, surface capping layer, and substrate material building blocks);

(2) Task 1.2 (TMD material building blocks); and

(3) Task 1.3 (structural, chemical and physical characterisation).

The material building blocks investigated in Tasks 1.1-1.3 are also being assessed for their electrical, optoelectronic and PEC properties in Tasks 1.4-1.5 of Work Package 1, but these findings are not included in this D1.1 report (they will be reported in D1.2 which is due in Month 26 of 40 in the project timeline).

Our ultimate objective is to take the achievements of the combined activities in WP 1 and WP 2 and create a PEC cell-to-system pathway to realise a PEC system in WP 3 and WP 4, respectively, that meets all the “high-risk / high-reward” objectives of the project to TRL 4 proof-of-concept verification. The challenges to achieving all of the objectives in the project are many and extremely difficult. To date, we have managed to make significant progress in all of the challenging areas, and we are still on course with a potentially feasible solution pathway at this timeline juncture. The high-risk nature of the project does not guarantee any level of end success of course, but we are encouraged by our progress to date, by our intermediate innovations, and by the confidential (sensitive) strategy presently being pursued, that utilises the knowledge gained from the investigations summarized by this D1.1 report and the related achievement of Milestone 2 to best position us to continue our advancement.

0. Introduction

The aim of all activities in WP 1 is to achieve the baseline building block component materials, structures and properties – as illustrated for TMDs in Figure 0.1, that will allow the consortium to ultimately create a fully integrated tandem PEC cell as illustrated in Figure 0.2 for large irradiation areas that will be formed in WP 2 and provided to WP 3 - WP 4 for the water-splitting system.

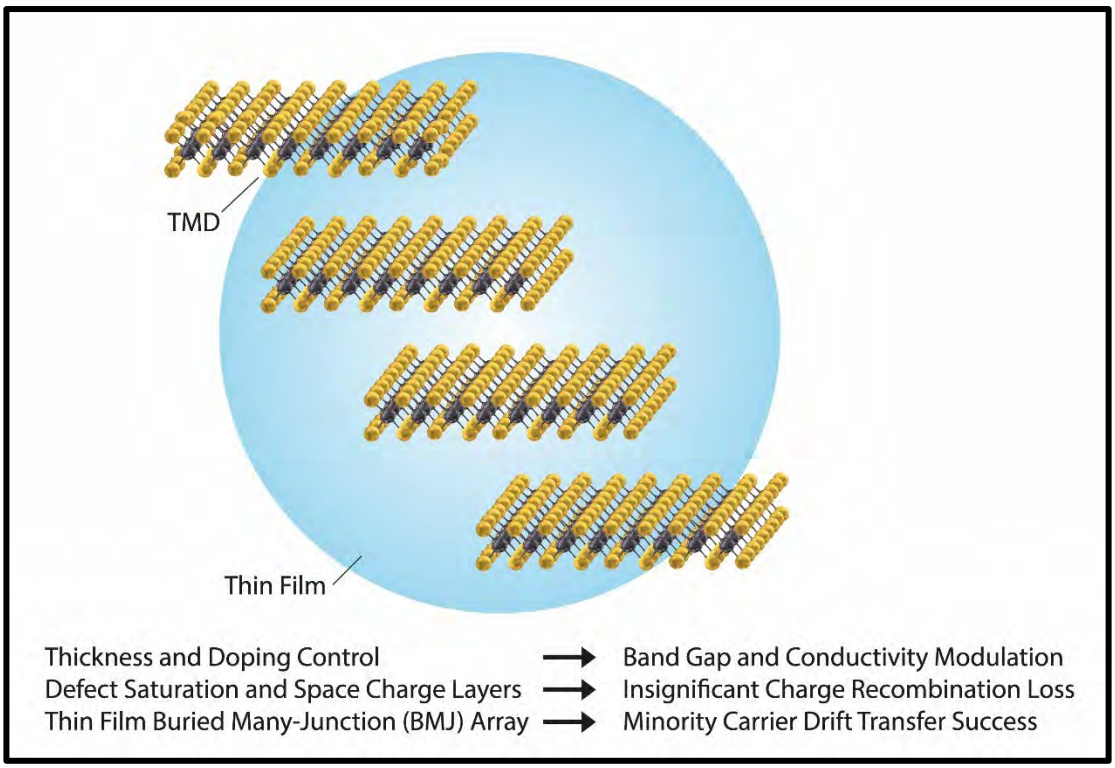

Figure 0.1: Illustrative schematic of material layer building block aims in WP 1 to achieve the WP 2 objectives.

We firstly must list in a public setting the achievements in terms of TCO and TMD material building blocks realised and investigated. Tables 1.1.1 (Task 1.1) and 2.1.1 (Task 1.2) list these building block TCO and TMD materials, respectively, investigated in WP 1 up to M24.

It is also necessary to show that the structural, chemical and physical assessments in Task 1.3 achieve the objective of confirming the formation of TCOs and TMDs, and also guide us in our building block selection process.

We will show that the TCO-based activities in WP 1 included here in D1.1 have permitted a broad investigation of building block TCOs for multijunction layers, for capping layers and for use as a substrate.

We will also show that the TMD-based activities in WP 1 included here in D1.1 have permitted a broad investigation of building block TMDs for multijunction absorber and pn-junction layers.

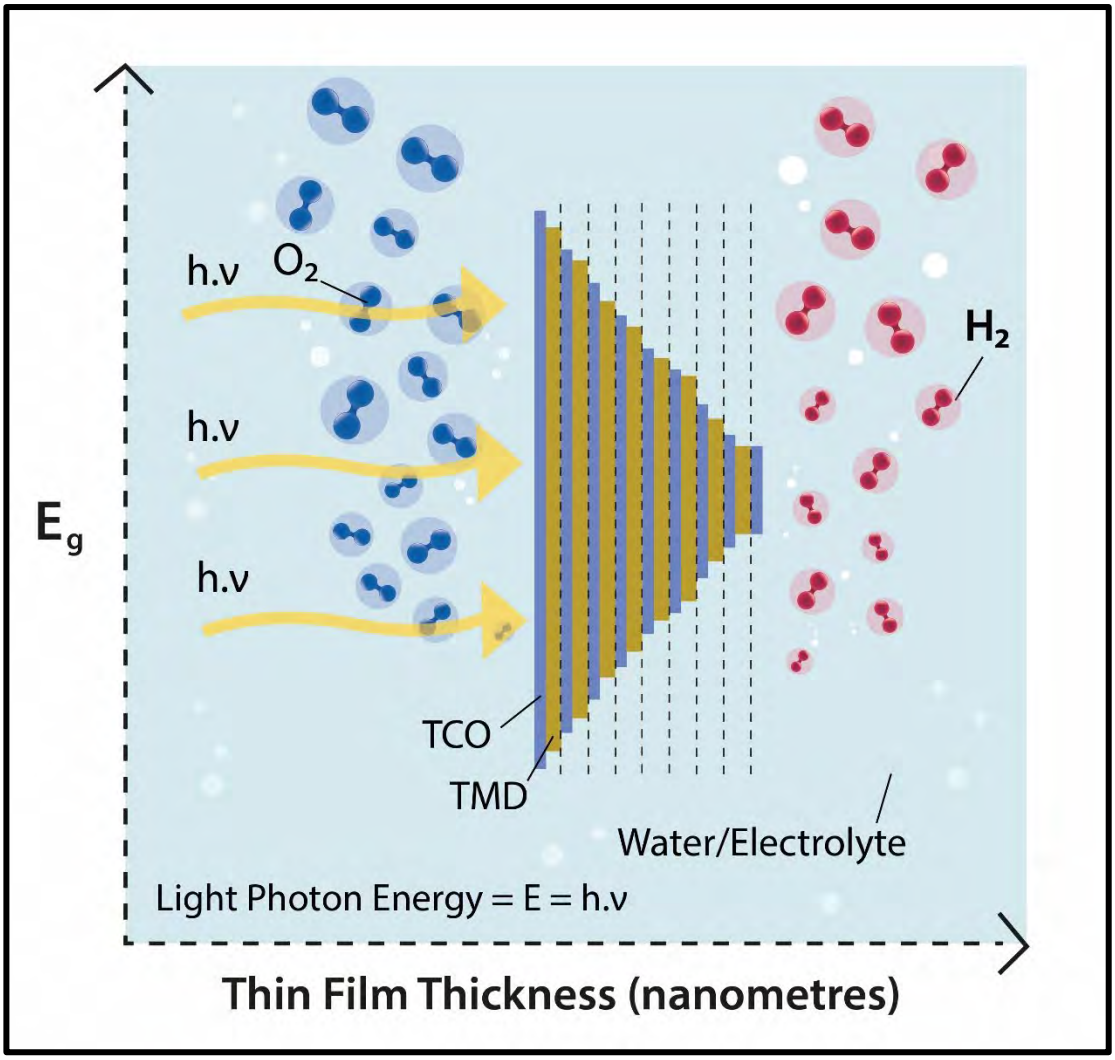

Figure 0.2: Illustrative schematic of the WP 2 objective in forming buried multijunction layers from the material building blocks of WP 1.

1. Task 1.1: TCO Material Building Blocks (layers, capping, substrate)

1.1 Introduction

Task 1.1 essentially focuses on assessing potential material building blocks for the TCO multijunction layers, the TCO surface capping layers, and the TCO substrate. It involves the partners AMO, CNR, and UCC, and it spans the period M1-M37 of the project 40-month timeline. The growth of TCOs is performed by using large-area (up to 200 / 300 mm diameter wafers) manufacturing-compatible, cost-effective technologies, such as ALD, CVD, and in some cases assisted by TAC-CVD, PVD, and co-sputtering. The aim is to grow both n-type and p-type TCO layers for the multijunctions, TCO capping layers for the semiconductor/electrolyte interfaces, and a thicker TCO layer for the cell substrate, all using environmentally-benign elements only – which is a significant challenge in itself.

It has to be underlined that the realization of p-type TCOs is a particularly challenging effort, so we have also decided to focus on TCOs spanning over a large range of workfunctions, to achieve large junction electric fields, necessary to separate the electron-hole pairs generated by photon absorption, thanks to the workfunction difference at the heterojunction. Another area of interest is the realization of thicker TCO layers to provide a conductive substrate for the realization of the active multi-junction PEC device. Careful attention is paid to the thermal budget alignment between the TCO growth processes and the TMD growth processes to ensure that the building block materials investigated are compatible for multijunction integration.

The overall focus is on low-cost, low temperature processing, and high performance, which in particular for TCOs means high optical transparency, high electrical conductivity, and the use of environmentally-benign and low-cost chemical elements, including in their delivery. The confidential list of studied materials is presented in Table 1.1.1 and includes almost forty different types or variants of TCO materials. In one case, a commercial TCO have been used as a test substrate or as a comparative substrate, particularly for Task 1.2 activities. The majority of TCOs investigated and listed in Table 1.1.1 are being explored for multijunction purposes, but some are also investigated to serve as capping layers (TCO-{1,3,22-27,36,37}) and substrates (TCO-{2,4,16,17,32,34,35,38,39}).

Table 1.1.1. TCO materials realised by the FreeHydroCells Consortium in the M1-M24 period.

Partner	TCO ID Material	Method	Substrate	Thickness Nominal (nm)	Type (NID, n, or p)
AMO	TCO-1	ALD	Glass	1-20	n
AMO	TCO-2	PVD	Glass	20-200	n
AMO	TCO-3	PVD	Glass	20	p
AMO	TCO-4	PVD	Glass	50-100	p
AMO	TCO-5	PVD	Glass	25-50	n
UCC	TCO-6	ALD	SiO2/Si	45	n
UCC	TCO-7	ALD	Sapphire	45	n
UCC	TCO-8	ALD	Quartz	45	n
UCC	TCO-9	ALD	SiO2/Si	50	p
UCC	TCO-10	ALD	Sapphire	50	p
UCC	TCO-11	ALD	Quartz	50	p
UCC	TCO-12	ALD	SiO2/Si	50	n
UCC	TCO-13	ALD	Glass	50	n
UCC	TCO-14	ALD	Glass	50	n
UCC	TCO-15	ALD	Sapphire	50	n
UCC	TCO-16	ALD	SiO2/Si	500	n
UCC	TCO-17	ALD	Glass	500	n
UCC	TCO-18	ALD	TMD/SiO2/Si	7	n
UCC	TCO-19	ALD	TMD/TCO/SiO2/Si	7	n
UCC	TCO-20	ALD	TMD/Sapphire	7	n
UCC	TCO-21	ALD	TMD/TCO/Sapphire	7	n
UCC	TCO-22	ALD	TMD/TCO/Glass	7	n
UCC	TCO-23	ALD	TMD/TCO/Glass	7	n
UCC	TCO-24	ALD	TMD/TCO/Glass	7	n
UCC	TCO-25	ALD	TMD/TCO/Glass	7	n
UCC	TCO-26	ALD	TMD/TCO/Glass	7	n

UCC	TCO-27	ALD	TMD/TCO/Glass	7	n
UCC	TCO-28	ALD	TMD/Glass	7	n
UCC	TCO-29	CVD-TAC	SiO2/Si	7	n
UCC	TCO-30	CVD-TAC	TMD/SiO2/Si	7	n
UCC	TCO-31	ALD	TMD/Sapphire	7	n
UCC	TCO-32	ALD	Glass	450	n
UCC	TCO-33	ALD	TMD/TCO/Glass	45	n
CNR	TCO-34	PVD	Glass	10-200	n
CNR	TCO-35	PVD	Glass	10-100	n
CNR	TCO-36	PVD	Glass	1-10	NID
CNR	TCO-37	PVD	Glass	1-10	NID
CNR	TCO-38	PVD	Glass	10-200	n
CNR	TCO-39	Commercial	TCO/Glass	650	n

1.2 Results and Discussion on TCOs

Activities across all three partners at AMO, CNR and UCC has spanned investigating TCOs for multijunction layers, capping layers and substrates. The literature is full of investigations on TCOs, such as FTO, ITO, TiO2, MoO3, etc. [1], and we explore many of these types of options.

TCO-1 is a well-established material for capping layers and a thickness of only few nanometers is reported often as sufficient, though the optimal value still needs to be experimentally determined in each case. We deposit TCO-1 in the range 1-20 nm by ALD processes.

Since the band gap is thickness-dependent for thin films in the nanometer range, AMO has performed optical characterization of TCO-1 films likely to be used as capping layers, from 3 to 15 nm, and found a band gap variation of 0.1 eV, as observed in Figure 1.2.1.

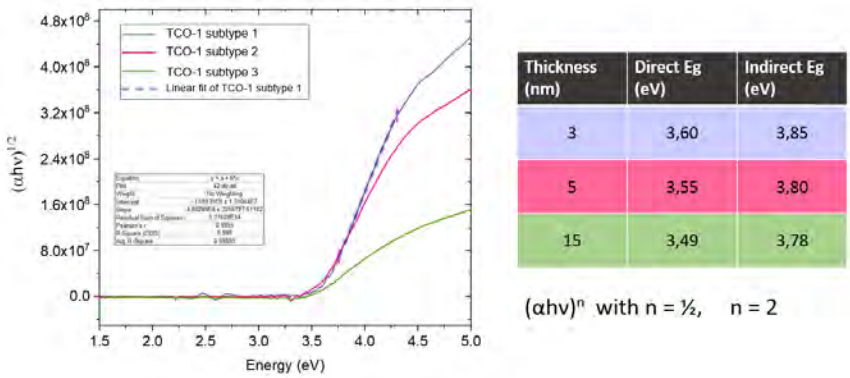

Figure 1.2.1: Tauc Plots and bandgap thickness dependence for TCO-1 by ALD, realised at AMO.

A major progress point in WP 1 was the development by AMO of deposition processes for TCO-3 and TCO-4, which are designated as p-type TCOs with different properties to each other. These material systems have potential uses as multijunction layers as well as surface capping layers. Other potential p-type TCOs have been investigated with different levels of

doping, but these have proven to result in n-type behaviour so far, although we are still investigating the possibility of them switching to being p-type with further contamination techniques.

Table 1.1.1 also reports the range of TCOs generated by UCC by methods such as ALD and CVD-TAC. Very significant progress has been made by UCC in advancing viable TCO building block options for the multijunction layers, the capping layers and the substrate material. UCC has also supplied a commercial TCO-39/glass for test and comparative substrates to all partners.

CNR has prepared various TCO building block materials (TCO-{34-39} in Table 1.2.1 below), all deposited by magnetron sputtering (PVD). In addition, CNR is using a TCO with a commercial material as the substrate for TMD deposition. Critical to the investigations of these TCOs are the properties of doping, conductivity and relative workfunctions.

While environmentally-benign elements and materials are the focus of the project for TCOs and all other material systems, we also recognize that some intermediate material systems may not meet this threshold and it may be necessary to use these materials or elements to achieve certain properties such as conductivity as we transition towards the end objective of the project, when we will use environmentally-benign materials and elements only.

2. Task 1.2: TMD Material Building Blocks (layers)

2.1 Introduction

The objective of T1.2 in WP 1 is to investigate and develop the TMD building block materials in the project that could potentially act as the main solar spectrum absorber in the PEC cells, in addition to forming TCO/TMD junctions and pn-multijunctions.

The literature presents a significant variety of TMD options, especially in the optical response area, with the MX2 stoichiometry, where M (the transition metal but including [mixed dopants]) could be W, Mo, Hf, Zr, [Nb], [Re], [Fe], [Mn], [Co], [Al], Pt, Pd and X could be S, Se or Te [2], and we explore many of these type of options.

Table 2.1.1 presents the list of TMD materials assessed in the project to date involving the partners UCC, AMO, RWTH, and CNR, which spans the FreeHydroCells project period M1-M37 of a total of 40 months. We grow or form non-intentionally doped (NID), n-type or p-type TMDs and we use environmentally-benign elements. These layers are formed on a whole variety of substrates depending on their experimental analysis purpose, such as glass, quartz, silicon, and TCO substrates, with area sizes from 1 cm x 1 cm up to 200 / 300mm wafers.

Critical issues are the nucleation and growth of TMDs on TCOs through various processing techniques, such as CVD, PVD, ALD, TAC-CVD, etc., with specifically targeted thicknesses, dopant densities and majority carrier types.

Table 2.1.1: TMDs materials prepared by the FreeHydroCells Consortium in the M1-M24 period.

Partner	TMD ID Material	Method	Substrate	Thickness Nominal (nm)	Type (NID, n, or p)
UCC	TMD-1	CVD-TAC	SiO2/Si	40	p

UCC	TMD-2	CVD-TAC	SiO2/Si	40	n
UCC	TMD-3	CVD	SiO2/Si	10	NID
UCC	TMD-4	CVD	TCO/SiO2/Si	10	NID
UCC	TMD-5	CVD	Sapphire	10	NID
UCC	TMD-6	CVD	TCO/Sapphire	10	NID
UCC	TMD-7	CVD	TCO/Glass	10	NID
UCC	TMD-8	CVD	TCO/Glass	10	NID
UCC	TMD-9	CVD	TCO/Glass	10	NID
UCC	TMD-10	CVD	TCO/Glass	10	NID
UCC	TMD-11	CVD	TCO/Glass	10	NID
UCC	TMD-12	CVD	TCO/Glass	10	NID
UCC	TMD-13	CVD	Glass	10	NID
UCC	TMD-14	CVD-TAC	SiO2/Si	40	NID
UCC	TMD-15	CVD-TAC	SiO2/Si	40	NID
UCC	TMD-16	CVD-TAC	Sapphire	40	NID
UCC	TMD-17	CVD-TAC	Sapphire	40	NID
UCC	TMD-18	CVD-TAC	Si	40	NID
UCC	TMD-19	CVD-TAC	Si	40	NID
UCC	TMD-20	CVD-TAC	SiO2/Si	40	n
UCC	TMD-21	CVD-TAC	SiO2/Si	40	n
UCC	TMD-22	CVD-TAC	SiO2/Si	40	n
UCC	TMD-23	CVD-TAC	SiO2/Si	40	n
UCC	TMD-24	CVD-TAC	SiO2/Si	40	n
UCC	TMD-25	CVD-TAC	SiO2/Si	40	n
UCC	TMD-26	CVD-TAC	SiO2/Si	40	p
UCC	TMD-27	CVD-TAC	SiO2/Si	40	p
UCC	TMD-28	CVD-TAC	SiO2/Si	40	p
UCC	TMD-29	CVD-TAC	Sapphire	40	n
UCC	TMD-30	CVD-TAC	Sapphire	40	n
UCC	TMD-31	CVD-TAC	Sapphire	40	n
UCC	TMD-32	CVD-TAC	Sapphire	40	n
UCC	TMD-33	CVD-TAC	Sapphire	40	n
UCC	TMD-34	CVD-TAC	Sapphire	40	n
UCC	TMD-35	CVD-TAC	Sapphire	40	p
UCC	TMD-36	CVD-TAC	Sapphire	40	p
UCC	TMD-37	CVD-TAC	Sapphire	40	p
UCC	TMD-38	CVD-TAC	Si	40	n
UCC	TMD-39	CVD-TAC	Si	40	n
UCC	TMD-40	CVD-TAC	Si	40	n
UCC	TMD-41	CVD-TAC	Si	40	n
UCC	TMD-42	CVD-TAC	Si	40	n
UCC	TMD-43	CVD-TAC	Si	40	n
UCC	TMD-44	CVD-TAC	Si	40	p
UCC	TMD-45	CVD-TAC	Si	40	p
UCC	TMD-46	CVD-TAC	Si	40	p
UCC	TMD-47	CVD	SiO2/Si, sapphire	10	NID

UCC	TMD-48	CVD	SiO2/Si, sapphire	10	p
RWTH	TMD-49	PVD-CVD-TAC	SiO2/Si, sapphire	3.8	NID, n, p
RWTH	TMD-50	PVD-CVD-TAC	SiO2/Si, sapphire	6.2	NID, n, p
RWTH	TMD-51	PVD-CVD-TAC	SiO2/Si, sapphire	8	NID, n, p
RWTH	TMD-52	PVD-CVD-TAC	SiO2/Si, sapphire	14.9	NID, n, p
RWTH	TMD-53	PVD-CVD-TAC	SiO2/Si, sapphire	4.3	NID, n, p
RWTH	TMD-54	PVD-CVD-TAC	SiO2/Si, sapphire	6.6	NID, n, p
RWTH	TMD-55	PVD-CVD-TAC	SiO2/Si, sapphire	11	NID, n, p
RWTH	TMD-56	PVD-CVD-TAC	SiO2/Si, sapphire	11.7	NID, n, p
CNR	TMD-57	Drop Casting	TCO-39/glass	1-3	p
CNR	TMD-58	Drop Casting	TCO-39/glass	1-3	p
CNR	TMD-59	Drop Casting	TCO-39/glass	1-3	p
CNR	TMD-60	Electrodeposition	TCO-39/glass	1-3	p

2.2 Results and Discussion on TMDs

The main objectives in the M1-M24 period for the TMD materials building block activity included growth and assessment of materials, and their most appropriate doping profiles for PEC cell applications. An appropriate growth process is the next consideration, which must permit moving from small area growth for analysis to large area growth for PEC cell applications. Processes should be feasible, low-cost, and careful consideration placed on thermal alignment compatibility.

As part of an initial, non-confidential doping assessment of typical TMD materials, UCC and all partners undertook a significant assessment of non-intentionally doped MoS_2 and WS_2, as well as their doped versions, p-type Nb-WS_2 and n-type Re-MoS_2. These were formed using TAC-CVD. We present in the next section the general structural, physical and chemical characteristics of these general material systems, and we assess the effect of the materials and the doping. We can present these material findings publicly as they are no longer part of our solution strategy plan.

In RWTH, TAC-CVD has been adopted to synthesize n-type TMD films of varying thickness, as well as to synthesize and optimise both n- and p- type TMD films, see Table 2.1.1. Different thickness of TMDs were grown followed by their structural and electrical characterization. The growth was carried out in a CVD furnace capable of handling standard 2 cm x 2 cm and 3 cm x 3 cm substrates (Fig. 2.2.1).

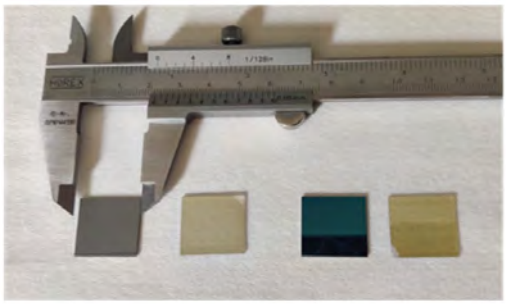

Figure 2.2.1. Various thickness of TAC-CVD TMD films on 2 cm x 2 cm substrates before and after sulfurization.

CNR is working on the formation of TMD films on TCO/Glass by Drop Casting and by Electrodeposition (Fig. 2.2.2).

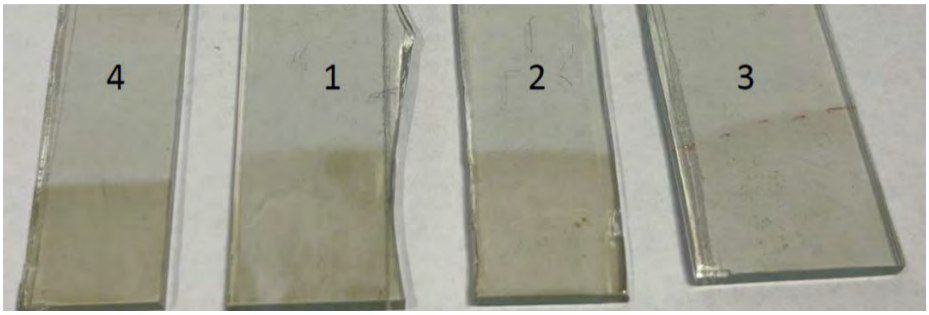

Figure 2.2.2. Electrodeposition TMD nanolayers formed on TCO/Glass.

3. Task 1.3: Structural, Chemical, Physical Characterisation

3.1 Introduction

The purpose of Task 1.3 in WP 1 is the structural, chemical, and physical characterisation of the building block TCO and TMD materials realized by the consortium in Tasks 1.1 and 1.2. The activity involves CNR, AMO, UCC, and RWTH, and the task spans the period M1-M37.

Numerous analytical techniques are used for this purpose by all involved partners, such as AFM, SEM, Spectroscopic Ellipsometry (SE), UV-VIS-NIR optical characterisation by reflectivity / transmissivity / external and internal quantum efficiency, Micro-Raman, PL, and FTIR. In addition, CNR also performs chemical and nanostructural characterisation by TEM/STEM in a facility equipped with a STEM/TEM machine with a 40-200kV Cold Field Emission Gun, 0.27 eV linewidth, Cs-corrector, 0.64 Å spatial resolution, BF/MAADF/HAADF STEM detectors, EDS detector with resolution 127 eV, and STEM EELS spectrum-imaging.

3.2 Results and Discussion

Figure 3.2.1 shows typical Tauc plots (extracted from the UV-Vis spectroscopy measurements) for two different forms of p-type TCOs, demonstrating the first with a more direct optical transition with higher band gap (typical values 2.3 – 2.7 eV), while the second type of TCO has a more indirect and lower band gap of (typical values 1.65 – 2 eV).

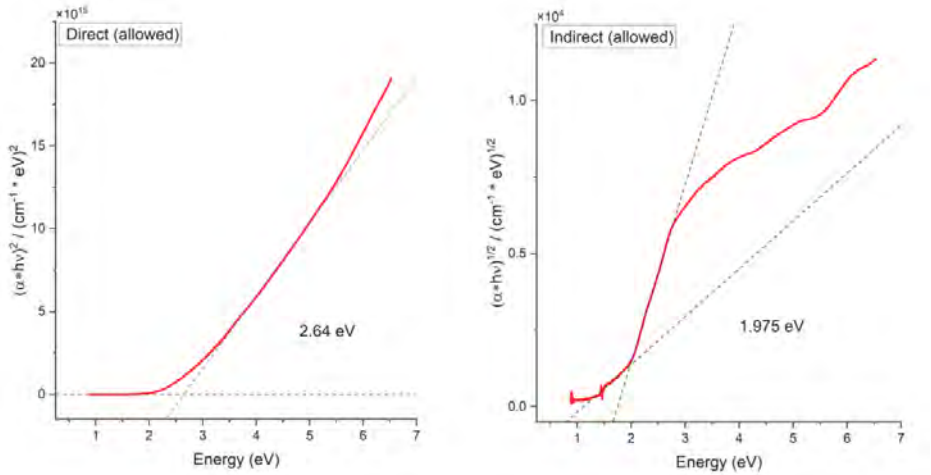

Figure 3.2.1: Tauc-Plots of two different p-type TCO forms with a thickness of ~20 nm, realised at AMO.

Figure 3.2.2 shows the Tauc-plot and SEM cross-section for an equivalent TCO thin to that in Figure 3.2.1, but this time with ~100 nm thickness, with a bandgap of 2.38 eV (left), as well as the AFM topography of the bare surface (right).

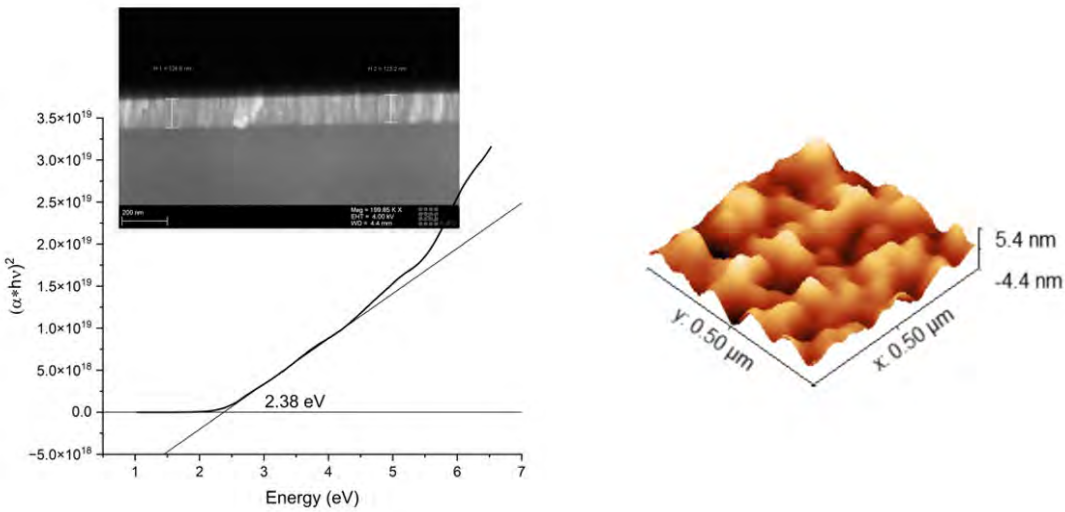

Fig 3.2.2: Structural and optical characterization of ~100 nm thick p-type TCO, realised by AMO (TCO-4), left: SEM, right: AFM topography.

AMO has also studied the growth of n-type TCO films (TCO-{1-2, 5}). Figure 3.2.3 summarizes the results of the structural, physical and optical characterization of such films deposited by RF sputtering. The films show promising optical properties: high transmissivity and low reflectivity, as well as a large band gap of 3.38 eV and high surface quality, with 1.95 nm RMS roughness. These properties indicate that the TCO material is a good candidate as an n-type junction material, as well as a TCO substrate material.

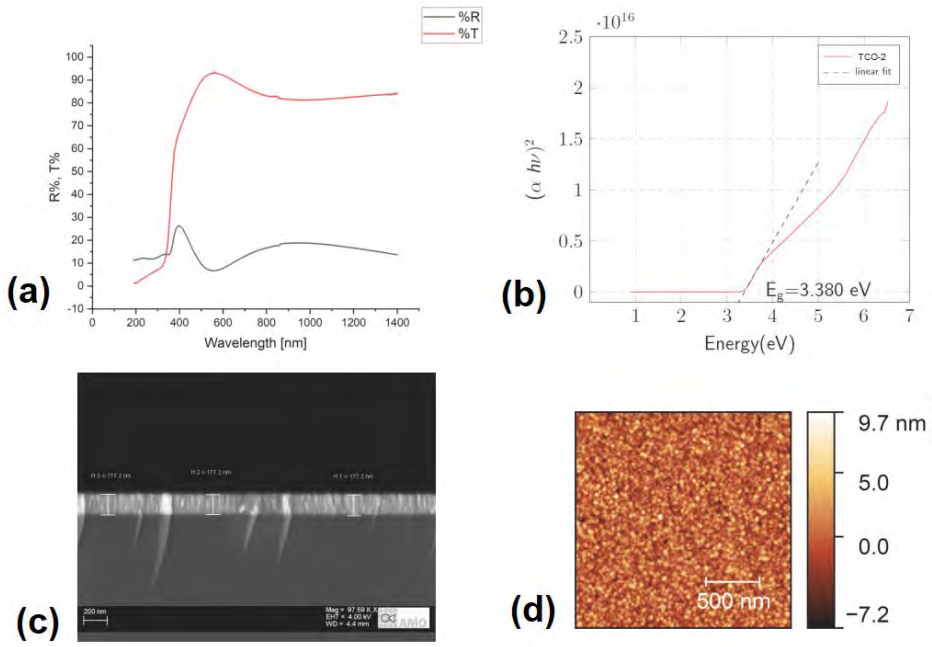

Fig 3.2.3. Characterisation of TCO-2 by AMO, for a 100 nm thin film. a) UV-Vis spectroscopy; b) Tauc plot with bandgap determined as 3.38 eV; c) SEM cross-sectional image; d) AFM scan of the surface.

In addition, the TCO material was characterized via Raman spectroscopy (Figure 3.2.4). The characteristic peak at approx. 433 cm^{-1} is shown to be present. Samples with varying O2 flow during sputtering were fabricated and their Raman spectra taken to evaluate possible improvement in thin film quality and composition. No significant influence on the structural properties was found and the final recipe does not include additional O2. A separate structural study investigated the influence of annealing time at a temperature of 400°C on the Raman signal. It was found that after 20 minutes of annealing, the Raman intensity decreases, indicating a decrease in thin film quality.

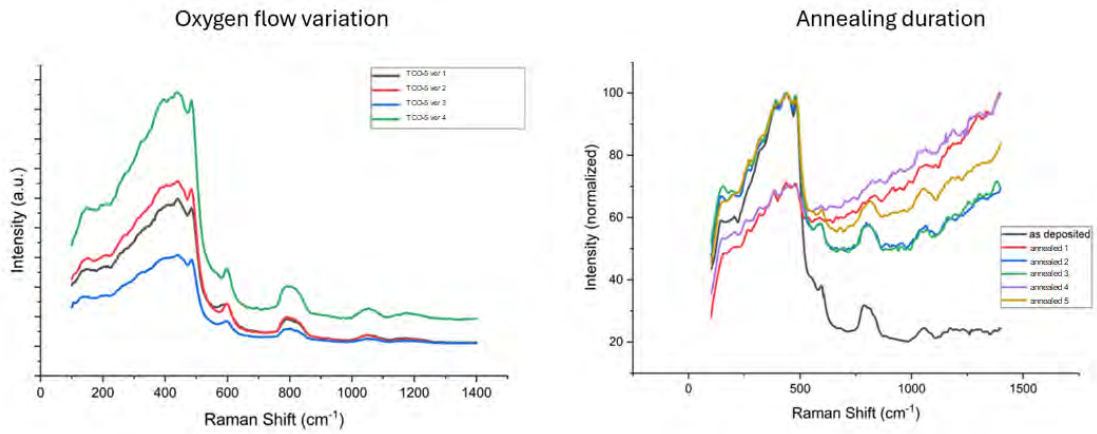

Figure 3.2.4: Raman spectra of TCO-5 thin films by AMO, for a 100 nm thin film. Left: changes in spectrum as O2 flow is introduced during sputtering. Right: changes in spectrum as the annealing time is increased.

At UCC, the non-intentionally doped MoS_2 (NID, TMD-14) and 5 %, 18 % doped MoS_2 (TMD-21 and TMD-25, respectively), as well as NID WS_2 (TMD-15) and 2 %, 4 % and 6 % doped WS_2 (TMD-{26,27,28}, respectively) TMD materials were assessed by Raman spectroscopy and X-ray diffraction, and these findings are reported in Figures 3.2.5 and 3.2.6, respectively [3]. The results in Figures 3.2.5 and 3.2.6 show signal lines that are well-known to be typical for such TMDs, confirming the formation of TMDs.

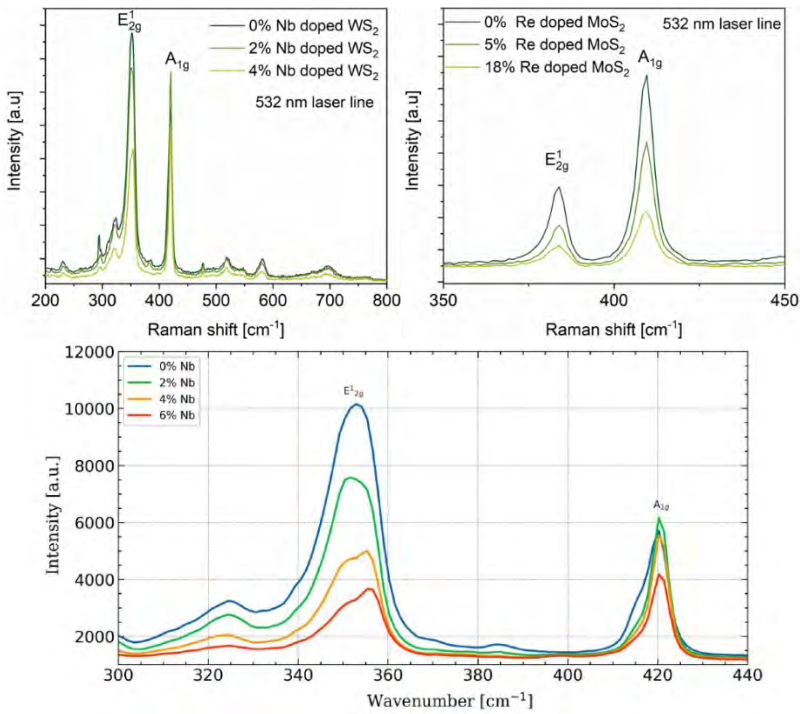

Figure 3.2.5: Raman spectroscopy findings for Nb-doped WS_2 and Re-doped MoS_2, confirming their TMD formation. Samples: non-intentionally doped MoS_2 (TMD-14) and 5 %, 18 % doped MoS_2 (TMD-21 and TMD-25, respectively); NID WS_2 (TMD-15) and 2 %, 4 % and 6 % doped WS_2 (TMD-{26,27,28}, respectively) TMD materials.

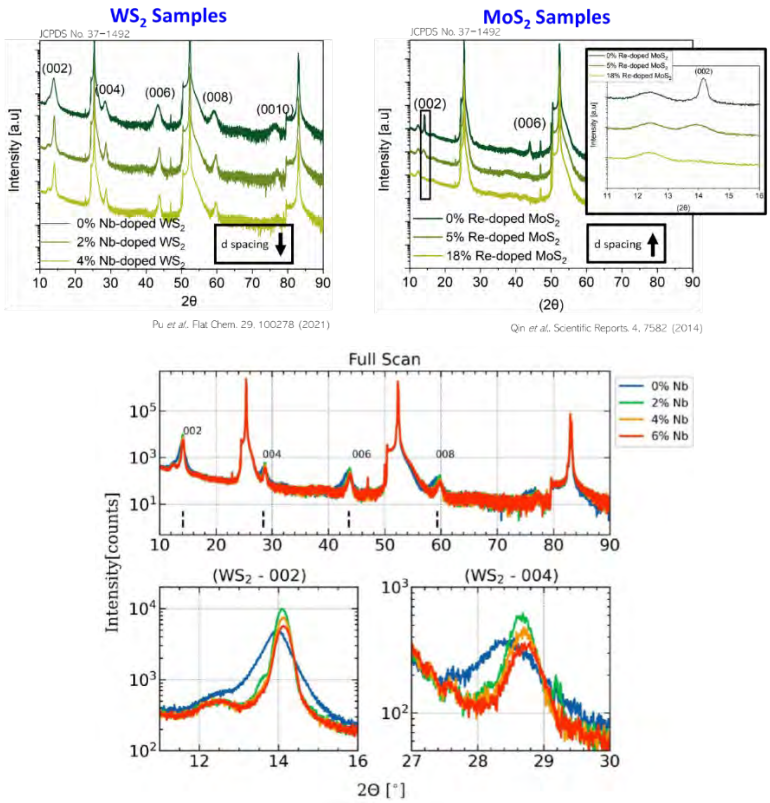

Figure 3.2.6: X-Ray Diffraction findings for Nb-doped WS_2 and Re-doped MoS_2, confirming their formation. Samples: non-intentionally doped MoS_2 (TMD-14) and 5 %, 18 % doped MoS_2 (TMD-21 and TMD-25, respectively); NID WS_2 (TMD-15) and 2 %, 4 % and 6 % doped WS_2 (TMD-{26,27,28}, respectively) TMD materials.

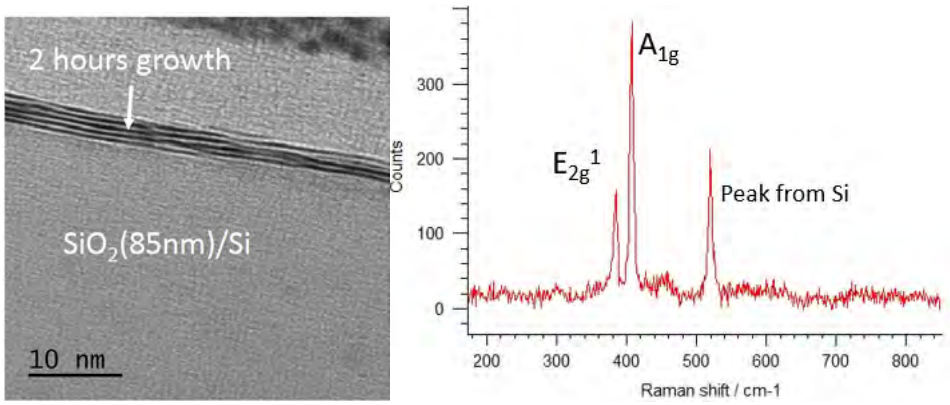

Figure 3.2.7: (left) High-resolution cross-sectional transmission electron microscopy micrograph and (right) Raman analysis, of large area manufacturing-compatible non-intentionally doped TMD-3 at UCC. The 2D layering (left) and the signals (right) confirm the formation of TMD.

Figure 3.2.7 (left) presents a cross-sectional transmission electron microscopy (TEM) micrograph of the small-to-large area NID transition process depositions towards realising large area TMD-3 film in a manufacturing-compatible 300 mm ALD kit as developed by UCC. The TEM micrograph (left) clearly shows the formation of 2D layered polycrystalline TMD, which is supported by the signals observed from the Raman spectroscopy (right).

In RWTH, various thicknesses of NID, n-type and p-type TMDs were obtained by CVD-TAC. These are designated as TMD-{49-52} and TMD-{53-56} in Table 2.1.1. AFM was implemented to analyse the surface morphology and roughness of all the TMD layers, with the thinnest NID nano TMD films, TCO-49 and TCO-53, shown in Figure 3.2.8 as general representation of the TMD responses. RMS roughness was measured to be around ~1-2 nm from the surface morphology of the majority of films.

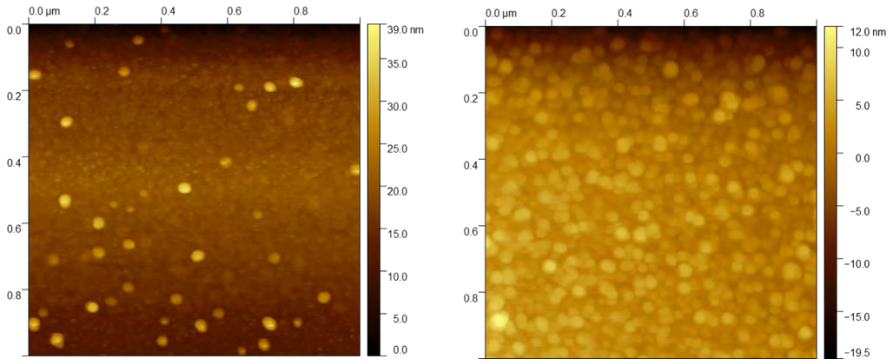

Figure 3.2.8. AFM images showing surface morphology of TCO-49 (left) and TCO-43 (right).

Micro-Raman characterization was carried out to analyse the quality and thickness of TMD films, and Figure 3.2.9 shows Raman characteristic peaks for TMD-{49-52} (left) and TMD-{53-56} (right). The positions of the A1g and E2g peaks for the left-hand set of TMD films were identified at 407.5 cm-1 and 382 cm-1, respectively, while for the right-hand set of TMD films, the A1g and E2g peaks were found to be at 419 cm-1 and 352 cm-1 respectively, all consistent with TMD formation.

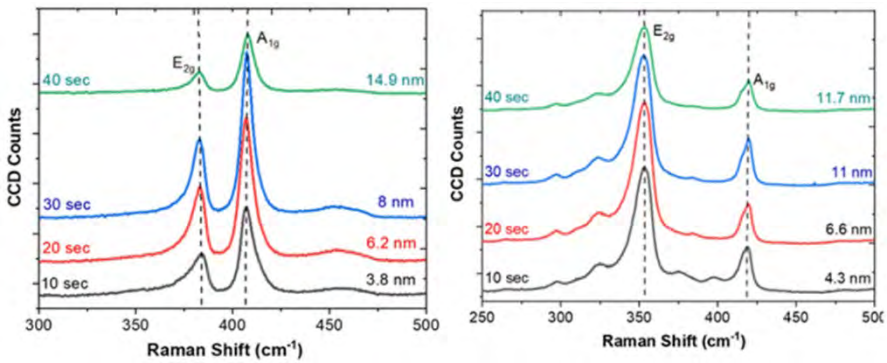

Figure 3.2.9. Raman spectra obtained for different thicknesses of TMD-{49-52} (left) and TMD-{53-56} (right).

In order to investigate thermal budget limitations for TMD film formation, a variant set of the TMD-49 and TMD-53 films in Table 2.1.1 were sulfurized at 550°C instead of 800°C, characterized and compared with the set sulfurized at 800°C. Figure 3.2.10 shows in NID, n-type or p-type pairs (bottom = 550°C, top = 800°C) the Raman spectra for the sulfurization temperature variant sets of TMD-49 and TMD-53 films. Similar thicknesses are compared in terms of NID, n-type and p-type for TMD-49, and the two differently processed NID of TMD-53 were compared, with the responses offset for comparison along the y-axis. It is clear from the signal responses that TMD films are formed for both thermal budgets.

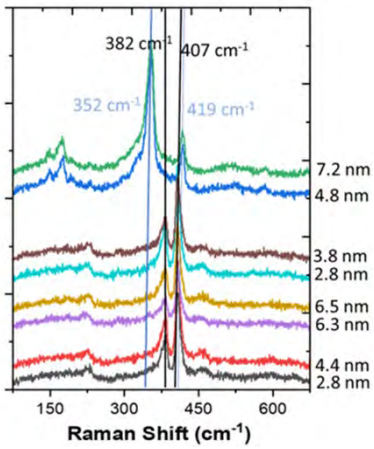

Figure 3.2.10: Raman spectra for NID, n-type or p-type pairs (bottom = 550°C, top = 800°C) of lower/higher temperature variant sets of TMD-49 and TMD-53 films. Similar thicknesses are compared in terms of NID, n-type and p-type for TMD-49, and the two differently processed NID of TMD-53 were compared, with the responses offset for comparison along the y-axis. It is clear from the characteristic signal responses that TMD films are formed for both thermal budgets.

The CNR activity on TMD growth focuses on the room temperature TMD deposition on TCO/Glass by Drop Casting and Electrodeposition. Fig. 3.2.11 reports cross-sectional FIB-SEM micrographs of TMD films deposited by Drop Casting on TCO/Glass. Approximately 10 nm of a TMD layer is formed on top of the TCO/Glass, although further optimization is needed.

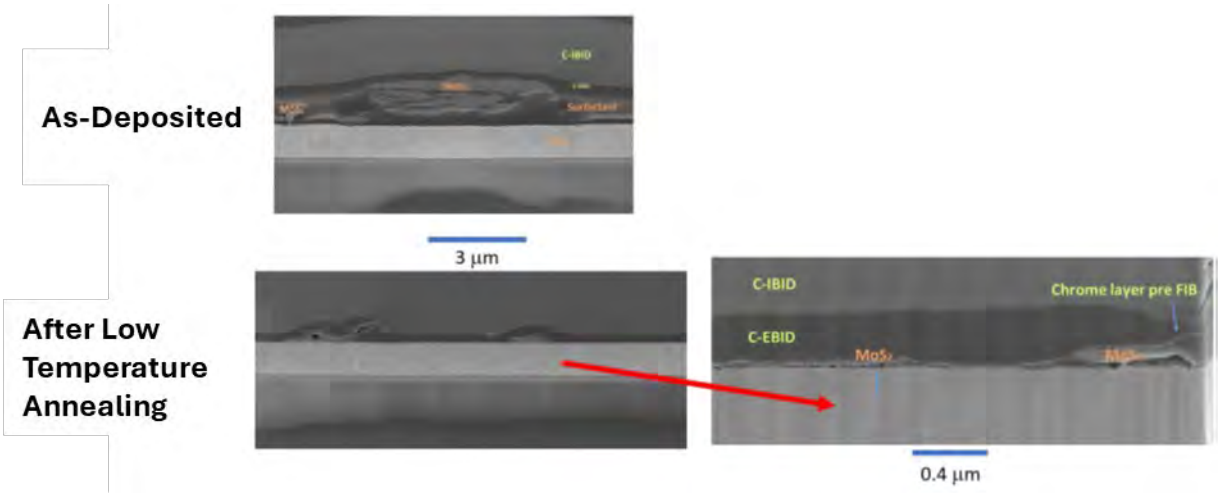

Figure 3.2.11. Cross-sectional FIB-SEM micrographs of TMD films deposited by Drop Casting on TCO/Glass (ID n.55) before (top), and after low temperature annealing.

A widely used tool for TMD sample characterization in CNR is the microRaman spectroscopy, usually performed with pump laser spot size of 1 um, power of 1 mW, and at 533 nm wavelength. Fig. 3.2.12 (top) shows an example of microRaman spectra taken TMD grown on FTO/Glass (TMD-{56,57,58}). The two lines at about 380 cm-1 and 405 cm-1 indicative of the TMD phase are clearly observed. A careful analysis of the line positions (Fig. 3.2.12 bottom) by following ref. [4] indicates that according to Raman all the CNR samples (TMD-{56,57,58}) on TCO/Glass are all p-type and subjected to tensile strain.

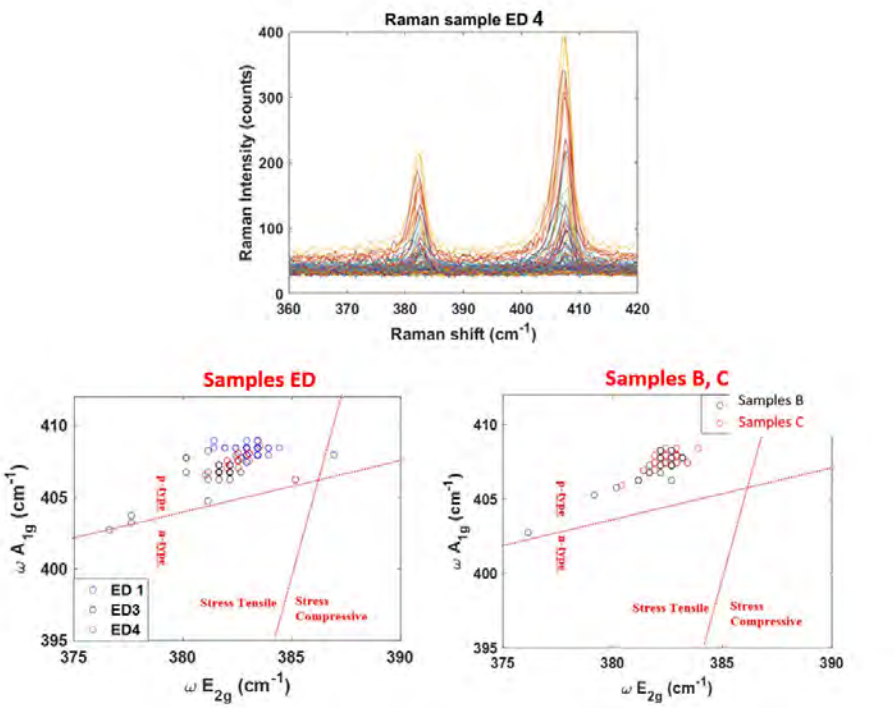

Figure 3.2.12. Top: microRaman spectra taken of the TMD layers grown by Electrodeposition on TCO/Glass (ID n.56, 57, 58). Bottom: from the analysis of the line positions, the CNR TMD samples on TCO/Glass are all p-type and subjected to tensile strain.

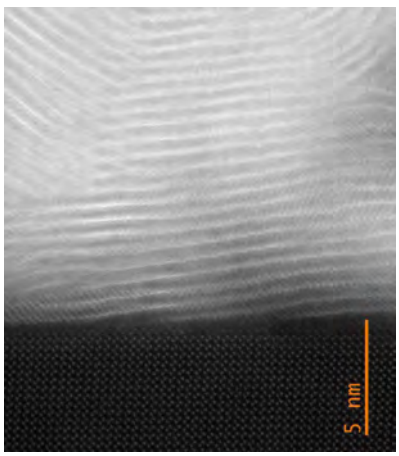

Figure 3.2.13. Cross-sectional high resolution scanning transmission electron microscopy (STEM) micrograph taken at CNR of a non-intentionally doped TMD/sapphire provided by partner UCC (TMD-16).

For the structural characterization CNR has provided to the consortium TEM / STEM analysis. As an example of such activity, Fig. 3.2.13 reports cross-sectional high resolution (HR) scanning transmission electron microscopy (STEM) micrographs of TCO-16 provided by partner UCC. The TMD appears with few defects and no precipitates, i.e., the TMD monolayers, clearly visible in HR, appear quite well-ordered.

4. Conclusions and Perspectives

Tables 1.1.1 (Task 1.1) and 2.1.1 (Task 1.2) list the building block TCO and TMD materials, respectively, investigated in WP 1 up to M24. The various assessments in Task 1.3 confirm the formation of TCOs and TMDs.

The TCO-based activities in WP 1 included here in D1.1 have permitted a broad investigation of building block TCOs for multijunction layers, for capping layers and for use as a substrate. Significant understanding has been achieved, and we have also made significant progress towards advancing building block selection in each of these objectives.

The TMD-based activities in WP 1 included here in D1.1 have permitted a broad investigation of building block TMDs for multijunction absorber and pn-junction layers. Significant understanding has been achieved regarding the influence of doping and other factors, and we have also made significant progress towards selecting the building block materials in this area of development.

We can conclude that the activities in WP 1 to date have served their purpose well and will continue to do so going forward, and we are continuing our work plan advancements in WP 1 and the related WP 2 on schedule and without deviation, which is a very significant achievement in a high-risk / high-reward project at M24 of the M40 timeline.

5. References

1. K. Ellmer, "**Past achievements and future challenges in the development of optically transparent electrodes**", *Nature Photonics* **6**, 809 (2012)

2. Anique Ahmed, Muhammad Zahir Iqbal, Alaa Dahshan, Sikandar Aftab, Hosameldin Helmy Hegazy and El Sayed Yousef, "**Recent advances in 2D transition metal dichalcogenide-based photodetectors: a review**", *Nanoscale* **16**, 2097 (2024)

3. Cansu Ilhan, Ievgen Nedrygailov, Ross Smith, Jun Lin, Christopher Kent, Ian M. Povey, Colm O'Dwyer, Salvatore Lombardo, Giuseppe Nicotra, Paul K. Hurley, Mick Morris, Dara Fitzpatrick, Justin D. Holmes and Scott Monaghan, "**Enhanced photoelectrochemical water splitting with doped transition metal dichalcogenide nanofilms**", *Materials Research Society (MRS) Fall Meeting, Symposium EN06: Emerging Energy Applications of Low-Dimensional Layered and Crystalline Materials: EN06.07.03 (1415-1430, 29/11/2023, Hynes, Level 3, Room 306)*, November 26 - December 1, 2023

4. Salvatore Ethan Panasci, Emanuela Schilirò, Giuseppe Greco, Marco Cannas, Franco M. Gelardi, Simonpietro Agnello, Fabrizio Roccaforte, and Filippo Giannazzo, "**Strain, Doping, and Electronic Transport of Large Area Monolayer MoS2 Exfoliated on Gold and Transferred to an Insulating Substrate**", *ACS Appl. Mater. Interfaces* **13**, 31248 (2021)

Appendices

Appendix 1: List of acronyms

AFM	=	Atomic force microscopy
CVD	=	Chemical vapor deposition
DC	=	Direct current
EELS	=	Electron energy loss spectroscopy
FTO	=	Fluorine doped Tin Oxide
ITO	=	Indium Tin Oxide
PEC	=	Photoelectrochemical
PL	=	Photoluminescence spectroscopy
PVD	=	Physical vapor deposition
RF	=	Radio frequency
TAC	=	Thermal Assisted Conversion
TCO	=	Transparent conductive oxide
TEM	=	Transmission electron microscopy
TMD	=	Transition metal dichalcogenide
SEM	=	Scanning electron microscopy
STEM	=	Scanning transmission electron microscopy
WP	=	Work Package
XRD	=	X-ray diffraction spectroscopy